

Theory of invasion extinction dynamics in minimal food webs

Jan O. Haerter, Namiko Mitarai, and Kim Sneppen

Center for Models of Life, Niels Bohr Institute, University of Copenhagen, Copenhagen, Denmark (Received 16 March 2017; revised manuscript received 25 September 2017; published 12 February 2018)

When food webs are exposed to species invasion, secondary extinction cascades may be set off. Although much work has gone into characterizing the structure of food webs, systematic predictions on their evolutionary dynamics are still scarce. Here we present a theoretical framework that predicts extinctions in terms of an alternating sequence of two basic processes: resource depletion by or competitive exclusion between consumers. We first propose a conceptual invasion extinction model (IEM) involving random fitness coefficients. We bolster this IEM by an analytical, recursive procedure for calculating idealized extinction cascades after any species addition and simulate the long-time evolution. Our procedure describes minimal food webs where each species interacts with only a single resource through the generalized Lotka-Volterra equations. For such food webs extinction cascades are determined uniquely and the system always relaxes to a stable steady state. The dynamics and scale invariant species life time resemble the behavior of the IEM, and correctly predict an upper limit for trophic levels as observed in the field.

DOI: [10.1103/PhysRevE.97.022404](https://doi.org/10.1103/PhysRevE.97.022404)**I. INTRODUCTION**

Biodiversity loss is a two-way road: Humans contribute to extinction of species and are reversely threatened by their loss [1]. Increasing global trade activity brings about worldwide mixing of species [2], by which alien species can be introduced to local communities [3]—at times resulting in profound changes to the populations of species or even eliminating them altogether [3,4]. Endemic species may hence experience extinction [5,6], especially when the change in biomass of one species cascades into the community, known as a trophic cascade [7–9], and eventually reshapes the entire community. At much longer time scales, new species may be introduced due to evolution and speciation, which may lead to either extinctions of existing or stable coexistence of all species, hence modifying biodiversity. Uncovering the basic rules of such a dynamics has challenged ecological research for decades and is a key to the understanding of ecosystem diversity and robustness [10].

A food web is the complex network formed by the relationships between all consumers and resources in a habitat. Among the few basic “laws” of food web ecology is the competitive exclusion principle [11,12], which states that when two consumers compete for the exact same resource or nonliving nutrient source, one consumer, e.g., the one growing more quickly, will eventually displace the other. This process hugely restricts stable coexistence of species. If, however, the faster grower is in turn limited by a predator, then sufficient resources can be left to the slower. In this sense, the existence of a species depends on other species further away in the food web. In the event of invasion, the new species may conflict with the competitive exclusion principle and its invasion may cause secondary, cascadelike, extinctions in other branches of the food web [13].

We recently showed that, despite the restrictions imposed by competitive exclusion, it is still possible to systemati-

cally construct a large and globally stable food web in a community. This was achieved through an exact method, using the generalized Lotka-Volterra (LV) equations without self-limiting terms for consumers [14]. Technically this was accomplished by adding species sequentially and ensuring that neither competitive exclusion [15] nor the feasibility of the existing species was violated. By “feasibility” it is here meant that there is a dynamically stable solution where all species populations are positive. Through this procedure, the constructed food web could obtain large species richness but tended to contain species on unrealistically high levels in the food web.

This paper studies the evolution of a simplified food web exposed to a series of random invasion events. First we propose the simple invasion extinction model (IEM), which is motivated by competitive exclusion, and we show that the IEM predicts a power-law distribution of species lifetime and an exponential distribution of extinction event size. We then analyze successful invasions and possible extinction cascades for a food web governed by the generalized LV equations. We prove that hierarchical food webs, i.e., treelike webs where each consumer has exactly one resource, will always collapse to a unique stable configuration of species, and we devise a recursive procedure for exactly calculating extinction cascades after the invasion by an arbitrary new species. When these food webs are evolved through many invasion attempts, they show the same dynamics as the IEM and predict a maximal number of trophic levels that resembles the four levels in real food webs. We finally place our assumption of hierarchical food webs in the context of empirical findings of link strength distributions and discuss the implications of our work in the context of biodiversity loss.

In our framework, the principle of competitive exclusion is strictly applied, and the invasion of a new species is completed after the system experiences a cascade of extinctions and reaches a new fixed point. Our bold simplification of one

resource per consumer allows us to develop a recursive procedure to analyze this limit exactly. The IEM, supported by the analysis of invasion and extinction dynamics in a treelike food web, provides analytical expressions of the species lifetime and the species extinction event size distribution, providing what is expected in this limit. Our theory thereby serves as another baseline to understand food webs in the real world.

II. THE INVASION EXTINCTION MODEL (IEM)

Consider a food web that only consists of two trophic levels, such as a microbial community of bacterial species at the basal and “predatory” virus species at the consumer level [16–18]. Competitive exclusion implies that species richness only increases if the basal species and their consumers increase one by one sequentially. It is straightforward to check that, if a consumer can feed on only one type of basal species, then the invasion by a new consumer can drive extinction of at most one competing consumer and in extreme cases its own resource species, but it cannot cause larger cascades. However, if a fast growing–slowly decaying basal species invades the system, any resident, more slowly growing, basal species and their respective consumers will all be driven to extinction. This has been previously simulated as a model of bacteria-virus ecosystems where interactions are described by generalized Lotka-Volterra equations [19]. A similar model was earlier explored in connection with virus and immune-system interactions [20].

The evolutionary dynamics of bacterial and phage species motivates us to propose a simple IEM of evolving random numbers, focusing on extinctions among basal species (Fig. 1): At any time step t , the IEM consists of a set of real numbers $r_i \in [r_{\min}, 1]$ representing decay rates (and/or inverse growth or “fitness” rates) of basal species. The real number $r_{\min} > 0$ thereby represents an assumed lower bound to any species’ decay rate while the upper limit of unity represents a normalized system carrying capacity. An invasion event corresponds to the introduction of one random number r_{new} that is uniformly drawn from the interval $[r_{\min}, 1]$. Initially, the set of resident species is empty, and hence any initial invasion will give a one-species community. r_{new} is always accepted, but any previous $r_i > r_{\text{new}}$ is removed from the set of resident species. In this simplified model the rate of removal for a given species is about $\Delta r \equiv r - r_{\min}$ per subsequent addition attempt. The overall probability $P(t)$ for a species to exist for exactly t addition attempts is

$$P(t) = \int_{r_{\min}}^1 dr \left(\frac{1-r}{1-r_{\min}} \right)^{t-1} \frac{r-r_{\min}}{1-r_{\min}} \sim \frac{1}{t(t+1)} \sim t^{-2}, \quad \text{for } t \gg 1. \quad (1)$$

The IEM further predicts the ensemble-averaged distribution of decay coefficients Δr to be proportional to $(1/\Delta r)[1 - \exp(-t\Delta r)]$, i.e., for long times $t \gg 1$, resident species are more likely to have large intrinsic fitness $1/\Delta r$. Further, for the long time limit, we obtain the extinction event size distribution, i.e. the probability $P(C)$ to witness C species becoming extinct after an invasion of one new species, to be exponentially

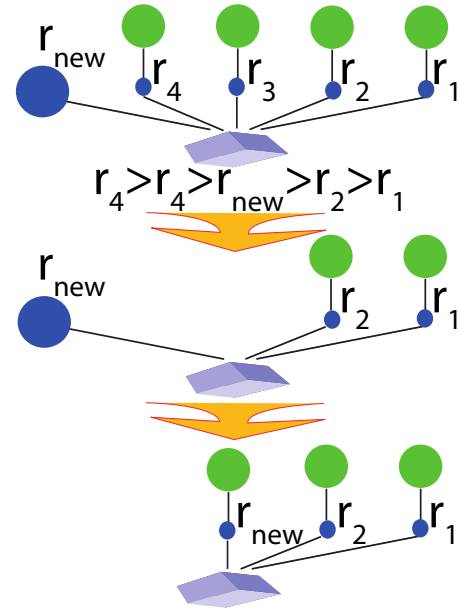


FIG. 1. Invasion extinction model. The schematic exemplifies the consequence of adding a species S_{new} with decay rate r_{new} at the basal level (blue circles). The blue shaded cube denotes the basic nutrient source, e.g., sugar. When adding S_{new} , all consumer-resource pairs (green and blue circles) corresponding to basal-level decay rates $r_i > r_{\text{new}}$ become eliminated; in the example these are the species N_3 and N_4 , corresponding to the decay coefficients r_3 and r_4 , respectively. Subsequently, a new level-two species may be added to N_{new} . This dynamics mimics species replacement as it would be seen in a dynamical implementation of the “kill the winner” scenario for microbial ecosystems [16].

distributed with typical size one, i.e.,

$$P(C) \approx \exp(-C)$$

(for more details, see Sec. A 1).

In the IEM the count of decay coefficients r_i , corresponding to the basal species richness, slowly increases, while most of the coefficients approach the lower threshold r_{\min} . As the count increases, the corresponding decay of biomass will, however, eventually conflict with the assumption of finite nutrient availability, which in our model is set by a total carrying capacity of unity. Accordingly, total species richness will not exceed $1/r_{\min}$.

The IEM does not reach steady state, since the fastest-growing basal species can be out-competed only by even faster growers, leading to persistent, albeit slow, “improvement” of fitness. However, the model can also be extended to take into account extinctions that go beyond this process of replacement by a species of higher fitness if one assumes that any coefficient can be eliminated at a small rate ϵ . Under those circumstances, both “fitnesses” and abundances reach a steady state, whereas the lifetime distribution $P(t) \propto \exp(-\epsilon t)/t^2$ acquires an exponential large- t cutoff. Such extinctions, which can also affect high fitness species, could, for example, be caused by an occasional predator that preys on two species and does so with different strength [19].

In summary, while the IEM makes several simplifying assumptions, e.g., the restriction to resource competition between

basal species, it does give a flavor of a complex evolutionary dynamics and allows us to analytically calculate the residence time distribution and the extinction event size distribution. In the following we explore a more realistic model of food webs, showing that the general dynamics of the IEM still hold there.

III. INVASION EXTINCTION DYNAMICS FOR A MINIMAL FOOD WEB

We now generalize the IEM to a more comprehensive food web model. This food web evolves from a single limiting nutrient source by sequential invasions of new species. We discuss the limit of rare invasions, where species invasions are sufficiently infrequent to allow the food web to reach a new steady state before a new invader arrives. The added species will prey on a random resident species, irrespective of the resident species' trophic level. This implies that there are no imposed limits to the maximum number of trophic levels; a possible upper limit will rather emerge as a prediction from the dynamical model. Importantly, we limit ourselves to the case where each new species \mathcal{N} consumes either a single resident species or the basic nutrient source. This restriction results in a "maximally trophically coherent" food web [21], where any species exclusively consumes other species at a specific level. It further constrains the network structure to be treelike with a "root" in the nutrient source. Equivalently, we will refer to this as a "hierarchical" food web.

For a species at a trophic level l , its relative change of biomass concentration is expressed as a function of all species $\mathbf{N} \equiv (N_1^{(1)}, \dots, N_i^{(l)}, \dots)$ as

$$\dot{N}_i^{(l)} / N_i^{(l)} = w_i^{(l)}(\mathbf{N}), \quad (2)$$

where the per capita growth rate $w_i^{(l)}(\mathbf{N})$ in the generalized Lotka-Volterra equations is a linear function of the other species' biomass concentrations [22,23]. At the basal level ($l = 1$) this flux includes competition for the nutrient source in terms of logistic growth

$$w_i^{(1)}(\mathbf{N}) \equiv \beta_i^{(1)} g \left(1 - \sum_{j=1}^{n_1} \frac{N_j^{(1)}}{K_j} \right) - \tilde{r}_i^{(1)} - \sum_{k=1}^{n_2} \tilde{\alpha}_{ki}^{(2,1)} N_k^{(2)}. \quad (3)$$

For higher trophic levels ($l > 1$)

$$w_k^{(l)}(\mathbf{N}) = \tilde{\beta}_k^{(l)} \tilde{\alpha}_{km}^{(l,l-1)} N_m^{(l-1)} - \tilde{r}_k^{(l)} - \sum_{p=1}^{n_{l+1}} \tilde{\alpha}_{pk}^{(l+1,l)} N_p^{(l+1)}. \quad (4)$$

Here $\beta_i^{(1)} g$ are the maximal growth rates of basal species, where $1/g$ represents the time scale and $\beta_i^{(1)}$ denotes a dimensionless factor that characterizes the difference of the growth rates among basal species. K_j is the carrying capacity for the basal species j . The coefficients $\tilde{r}_i^{(l)}$ denote decay (or death) rates, $\tilde{\beta}_k^{(l)}$ is the dimensionless consumption efficiency of a species k at trophic level l , and $\tilde{\alpha}_{km}^{(l,l-1)}$ are interaction strengths, which vanish when there is no interaction. The trophic level l may vary between unity at the basal level, consisting of primary producers, to the level L , which is the top trophic level, consisting, e.g., of large predators. For top species, that is,

those that have no consumers, the loss term in $w_k^{(l)}(\mathbf{N})$ only contains the intrinsic decay rate $\tilde{r}_k^{(l)}$. The lack of summation in the first term for the equation for a consumer reflects that the consumer k at level l feeds on only one resource species (m) at level $l - 1$.

We then cast the equations in dimensionless form, by measuring time in units of $1/g$, normalizing the biomasses of the basal species j by K_j , and normalizing the consumer k at the trophic level l by $g/\alpha_{km}^{(l,l-1)}$. This results in the equations

$$w_i^{(1)}(\mathbf{N}) \equiv \beta_i^{(1)} \left[1 - \sum_{j=1}^{n_1} N_j^{(1)} \right] - r_i^{(1)} - \sum_{k=1}^{n_2} \alpha_{ki}^{(2,1)} N_k^{(2)}, \quad (5)$$

for $l = 1$, and for higher trophic levels ($l > 1$),

$$w_k^{(l)}(\mathbf{N}) = \beta_k^{(l)} N_m^{(l-1)} - r_k^{(l)} - \sum_{p=1}^{n_{l+1}} \alpha_{pk}^{(l+1,l)} \cdot N_p^{(l+1)}, \quad (6)$$

with rescaled parameters $r_i^{(l)} \equiv \tilde{r}_i^{(l)}/g$, $\beta_k^{(2)} \equiv \frac{\alpha_{km}^{(2,1)}}{g/K_m} \tilde{\beta}_k^{(2)}$, $\beta_k^{(l)} \equiv \frac{\alpha_{km}^{(l,l-1)}}{\alpha_{mi}^{(l,l-1)}} \tilde{\beta}_k^{(l)}$ for $l \geq 3$, and the rescaled interaction strength $\alpha_{ki}^{(l,l-1)}$ takes the value of either zero or 1. We perform the analysis using this general dimensionless form and later discuss plausible parameter values.

When the species interactions are governed by the generalized LV equations [Eqs. (2)–(6)], stable coexistence for the food web structure must satisfy the *food web assembly rules* [15] in order for the nontrivial steady state $w_i(\mathbf{N}) = 0$ to have a unique solution. These rules can easily be summarized by visualizing the graph of a food web, consisting of all species and their interaction links. One then considers a *nonoverlapping pairing* of interacting species, which results when each species is thought of as "paired" with exactly one other species and each species must be involved in exactly one such pair. Nutrient sources may, but need not, be involved in the pairing. The rule of nonoverlapping pairing secures that there is no competitive exclusion [15]. When the graph is a tree, it can be checked that the successful pairing is unique.

When a web fulfills the structural requirement associated to competitive exclusion, it may still do so while giving (unrealistic) solutions to the LV equations where some species populations are negative. The additional requirement of only positive species populations is referred to as "feasibility." For a treelike food web that fulfills the pairing rule (Fig. 2), it has been proven that a feasible solution is globally stable, and a method to find a parameter set that gives a feasible solution has been provided [14]. For later use, we refer to the consumer (resource) within the pair as *free (controlled)* [14,15]. As mentioned above, species without consumers are referred to as *top species*, which are of course always free.

It is worth noting that the nonoverlapping pairing mathematically results from the condition that $\det R \neq 0$ with R the interaction matrix, and the same topological constraint can be obtained by the first part of Levin's loop analysis [24] when applied to a tree food web. Global stability of the tree food web ensures the linear stability that is the focus of Levin's approach, and hence it also satisfies the criteria for the sign for the coefficients in the Levin loop analysis.

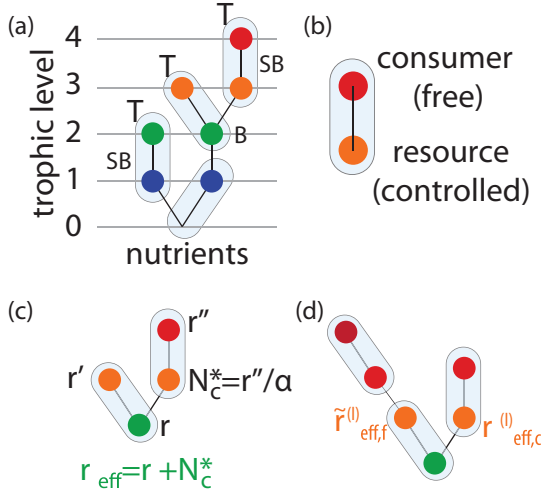


FIG. 2. Definitions. (a) Simple food web consisting of four trophic levels. We define the nutrient source to be trophic level zero. The trophic level of any species is the average trophic level of its resources plus 1. Colored circles mark species, light blue ovals mark pairings of species, and symbol (T) marks the top species, i.e., species without consumers. Side branches are marked by the symbol “SB.” A branching species (or branching point) is marked by “B.” $N_c^* = r''/\beta$. (b) An example of a pairing, consisting of a “free” consumer and a “controlled” resource species. (c) Definition of r_{eff} for a controlled species: r_{eff} equals the sum of the decay coefficient of the species itself and the steady-state density of its controlled consumer(s). (d) Illustration of the condition for feasibility at branching points, showing the comparison between $\tilde{r}_{\text{eff},f}^{(l)}$ and $r_{\text{eff},c}^{(l)}$ for two branches formed by a free, respectively controlled, species. (Figure reproduced from the literature [14].)

A. Evolution of a food web

We now turn to the actual evolution of our food webs, using the LV model just described. For simplicity, the selection of prey by an invader is taken to be entirely random, that is, any resident species is selected at equal probability. Plausible variants, such as using weighting of probabilities by species concentrations, caused no modifications to the conclusions drawn here. When an invader enters an existing community, this can be seen as a small population of the invader being added and the resulting food web integrated until a new steady state is reached. An example is shown in Figs. 3(a) and 3(b), where the integration was carried out numerically. Before the addition [Figs. 3(a) and 3(b), left] and after the transient readjustment of species concentrations [Fig. 3(a) and 3(b), right], the species with positive populations fulfill the food web assembly rules, while the transient [Figs. 3(a), center, and 3(b)] is characterized by a cascade of extinctions.

While it is in principle possible to carry out such integrations for a large number of invasion events and thereby obtain a numerical simulation of long-term evolution, it is more instructive to look for a systematic procedure by which invader species cause restructuring of the existing community. In the following we show that such a procedure indeed exists by first demonstrating that the steady state of a community is always unique and globally stable. Second, we give a recursive method

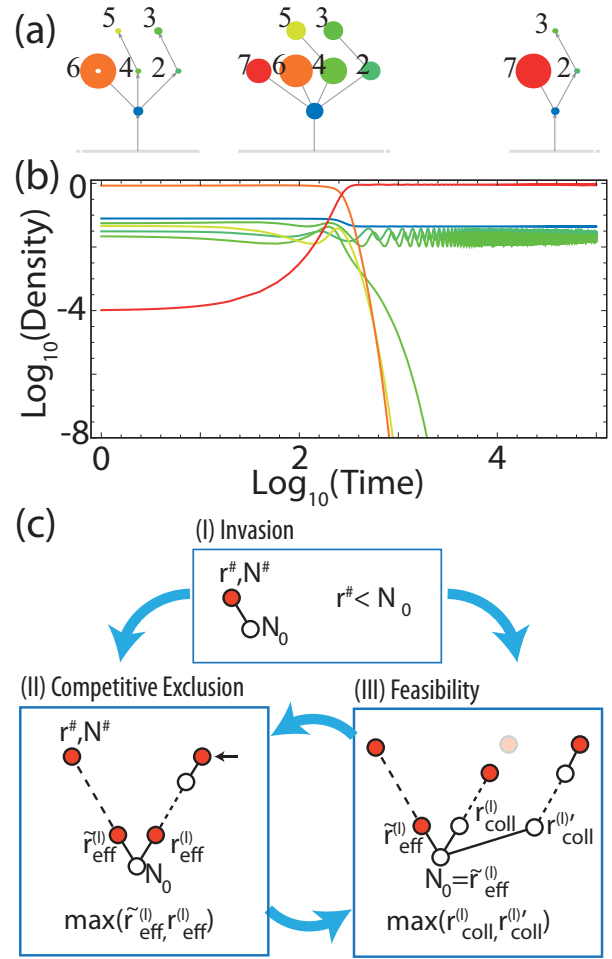


FIG. 3. Rules for invasions and species extinctions. (a) Introduction of new species (labeled “7”) eliminates species 6 and 4 by competitive exclusion and species 5 by resource depletion (since $r_7 < r_6$ and $r_7 < r_4$). The node area in the left and right schematic is proportional to species concentrations; in the central schematic, the node area is proportional to the species’ decay coefficients r_i . Colors reflect the time of species addition (blue is historic, red is recent). (b) Simulated population dynamics with extinction of species 4, 5, and 6. (c) Invasion rules emphasizing the iterative elimination process: (I) invasion by a new species, (II) competitive exclusion, and (III) feasibility. The definitions of decay rates in (c) are as follows: $r_{\text{eff}}^{(l)} \equiv [r^{(l)} + \sum_c N_c^{*(l+1)}]/\beta^{(l)}$, where the controlled species concentrations $N_c^{*(l+1)}$ are determined from Eq. (6); $r_{\text{coll},c}^{(l)} \equiv r_{\text{eff},c}^{(l)} + r_{\text{coll},f}^{(l+1)}/\beta^{(l)}$; $r_{\text{coll},f}^{(l)} \equiv \max(r_{\text{coll},c,1}^{(l+1)}, \dots, r_{\text{coll},c,n}^{(l+1)})$.

for determining the new steady state after an invasion event has taken place.

1. Uniqueness and stability of the steady state

On a random invasion to a treelike food web, either the nonoverlapping pairing or the feasibility of the steady state can be violated. In such a case, if there is a steady state solution $\mathbf{N} = \mathbf{N}^*$ that satisfies:

$$\begin{aligned} \text{If } N_i^{*(l)} > 0 \text{ then } w_i^{(l)}(\mathbf{N}) &= 0, \\ \text{otherwise } N_j^{*(l)} = 0 \text{ and } w_j^{(l)}(\mathbf{N}) &\leq 0, \end{aligned} \quad (7)$$

then it is globally stable, because

$$V(\mathbf{N}) = \sum_{l=1}^L \sum_i c_i^{(l)} [N_i^{(l)} - N_i^{*(l)} \ln N_i^{(l)}] \quad (8)$$

with

$$c_i^{(1)} = 1/\beta_i^{(1)}, \quad c_k^{(l)} = c_m^{(l-1)}/\beta_k^{(l)},$$

[see Eq. (6) for indices] is a Lyapunov function [22] for $\mathbf{N} \geq 0$:

$$\begin{aligned} \frac{d}{dt} V(\mathbf{N}) = & - \left[\sum_{i \text{ with } N_i^{*(1)} > 0} (N_i^{(1)} - N_i^{*(1)}) \right]^2 \\ & + \sum_{j,l \text{ with } N_j^{*(l)} = 0} \frac{1}{\beta_j^{(l)}} N_j^{(l)} w_j^{(l)}(\mathbf{N}^*) \leq 0, \quad (9) \end{aligned}$$

and $\mathbf{N} = \mathbf{N}^*$ satisfies the equality. Intuitively, $V(\mathbf{N})$ can be thought of as a measure of the “distance” from steady state, a sustained decrease in V hence corresponds to a sustained approach towards the steady-state species concentrations. To see that $dV(\mathbf{N})/dt$ is not positive, we note that the last term in Eq. (9) only contains species j, l which have zero population at steady state stabilized by $w_j^{(l)}(\mathbf{N}^*) \leq 0$ [see Eq. (7)]. This means that if we find a steady-state solution that satisfies Eq. (7), then it uniquely identifies the species j that is driven to extinction ($\{N_j^{*(l)} = 0 \text{ and } w_j^{(l)}(\mathbf{N}^*) \leq 0\} \Rightarrow N_j^{(l)} = 0$).

2. Recursive determination of the steady state

Given the uniqueness and stability of a steady-state solution, we now only lack a procedure that allows us to find the steady state. We hereby describe the recursive procedure to determine how a food web will react to an invasion event by a new species \mathcal{N} that feeds on a single resident species. The outline is as follows: Thanks to the linearity of the equation $w(\mathbf{N}) = 0$ in all species biomasses \mathbf{N} , it is possible to analytically determine the possible change of the fixed point affected by the new invader one by one and calculate the steady-state value of the biomass exactly. This allows us to find the species that should go extinct. By removing all of these we can obtain the new, feasible, and globally stable steady state that satisfies the condition expressed in Eq. (7), which the Lyapunov function [Eq. (8)] guarantees to be the final state after the transient period. Specifically, the following method allows us to analytically find the final state without explicit (time consuming) integration of Eq. (2) after species addition.

(I) *Invasion.* On invasion by a species $N^\#$ with decay rate $r^\#$ and consumption efficiency $\beta^\#$, there is no consumer for the new species $\mathcal{N}^\#$. Accordingly, $\mathcal{N}^\#$ initially grows if its decay coefficient $r^\#$ is less than the concentration of its prey N_0 times $\beta^\#$. In case of the basal species, it can easily be checked that N_0 should instead be replaced with $[1 - \sum_{j=1}^{n_1} N_j^{(1)}]$. For sufficiently small $r^\#$, possible conflicts are recursively resolved by removal of species. Such conflicts can arise directly, when competitive exclusion is present [Fig. 3(c,II)], or indirectly, when feasibility is violated [Fig. 3(c,III)].

(II) *Competitive exclusion.* When an invader leads to violation of competitive exclusion, or, equivalently, the pairing rule, then either the species itself or one or several other species

have to be removed. The test for removal starts by considering subsequent branching points as one moves down the food chain from the new species. Because pairing was violated, there is at least one branching point that separates two free species. Let us assume that this branching point has level $l - 1$. One now has to compare the effective decay coefficients $r_{\text{eff}}^{(l)}$ for the two free species above the branching point. These are each given by

$$r_{\text{eff},i}^{(l)} = \left(r_i^{(l)} + \sum_c N_c^{*(l+1)} \right) / \beta_i^{(l)}. \quad (10)$$

Here the effective decay rate of the free species i at level l takes into account predation by the controlled species, marked by the subscript c , that consume the given species i . The biomass of these predators N^* is determined recursively from the top species as $N_c^{*(l)} = r_{\text{eff}}^{(l+1)}$, where $r_{\text{eff}}^{(l+1)}$ is the effective decay rate of the free species feeding on the given controlled species [from $w_i^{(l+1)}(\mathbf{N}) = 0$ in Eq. (6)]. Between the two competing free species, the one corresponding to the smaller effective decay rate will prevail and the top species on the other branch will be removed. This is in parallel to the resource-ratio hypothesis [25,26], which states that when two species compete for a single resource, the species that requires less of the resource for its survival in the equilibrium state would out-compete the other species: Here, the resource is the controlled species biomass at the branching point, and $r_{\text{eff}}^{(l+1)}$ denotes the resource required by the two competing free species.

(III) *Feasibility.* Once nonoverlapping pairing is satisfied, one needs to check for feasibility [Fig. 3(c,III)]. Violation of feasibility can appear due to indirect interaction between species at a branching point, where the branching point includes a controlled species or branch. The biomass of the branching point equals the effective decay rate of its paired free species, $N_0 = \tilde{r}_{\text{eff}}$. This now limits the free species’ biomass on any controlled branch. If there are several controlled branches above the branching point, then they are compared through their *collective decay rate* $r_{\text{coll},c}^{(l)}$ (for more details, see Sec. A2), see Fig. 3(c,II) (derivations are given in next subsection). If $r_{\text{coll},c}^{(l)} > \tilde{r}_{\text{eff}}^{(l)}$, then the top species of the corresponding branch has a negative concentration and is removed. If there is more than one controlled branch that satisfies the condition, then the top species of the branch with the largest $r_{\text{coll},c}^{(l)}$ is removed first.

Alternating the two types of removal (II) and (III) recursively systematically determines how species are sequentially removed by competitive exclusion, caused by a newly emerging top predator, and by feasibility of top species that weakens their supply food chain, respectively. This is illustrated by the cycle in Fig. 3(c).

Extinctions may hence lead to other extinction events far away in the food web. The food web is relaxed when the nutrient source has been reached and all conflicts remedied. The resulting network again has a tree structure and is dynamically stable as well as feasible. As our recursion only eliminates species with $N_j^{*(l)} = 0$ and this in itself cannot disturb the remaining species with $N^* = 0$, the above recursion exactly removes the species specified by the unique solution of Eq. (7).

This procedure allows us to simulate a sequence of invasions and potential subsequent extinctions. Notably, no explicit numerical integration of the time evolution is required. Our

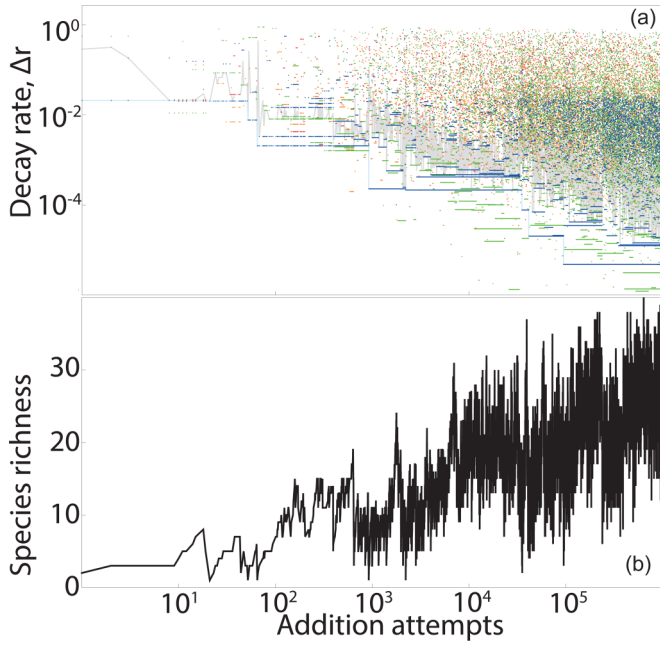


FIG. 4. Evolution of fitness and diversity. (a) Decay rate $\Delta r \equiv r - r_{\min}$ for all species vs. time in units of invasion attempts using $r_{\min} = 0.02$. Blue, green, orange, and red points mark the presence of a species at trophic levels 1, 2, 3, and 4. The blue line marks the lowest decay coefficient at the basal level. The gray line marks the median decay rate; note its increase whenever a new superior bottom species appears. Note the double-logarithmic scales. (b) Total species richness vs. time.

methodology is systematic and yields unique solutions, and we prove that the time evolution after any invasion attempt follows a globally stable trajectory.

B. Results

Using our methodology, we can now simulate millions of invasion attempts and avoid “numerical extinctions” due to numerically small population sizes or overall high computational effort. For simplicity, in the simulation we set $\beta_i^{(l)} = 1$ and use the decay rates $r_i^{(l)}$ to characterize the intrinsic species fitness. We further comment on the choice of consumption efficiency in Sec. A3. As in the introductory two-level IEM, decay rates are always chosen randomly from a uniform distribution between r_{\min} and 1. The evolution of the species’ intrinsic fitness [Fig. 4(a)], accompanied by a general increase in species richness [Fig. 4(b)], shows a stepwise decline in the lowest values of decay coefficients, i.e., monotonic increase of maximal intrinsic fitness. This feature is most clearly visible for basal species (shown in blue). Note that whenever the lowest decay coefficient for a basal species declines, all other decay coefficients (i.e., species) are also eliminated. These increasingly rare events of invasion by a globally superior basal level species are each followed by self-similar optimizations of the subsequently adapted occupation of other niches.

Notably, despite the greater network complexity of the multilevel model, the gradual increase in species richness [Fig. 4(b)] still resembles the behavior of the simple two-level

IEM. The resulting fractal-like evolution of the food web can be illustrated in terms of the origination-extinction matrix [Figs. 5(a) and 5(b)], where we highlight the pronounced self-similarity at different temporal scales [comparison of Figs. 5(a) and 5(b)]. Similar matrices were also used for the characterization of macroevolution on palaeontological time scales [27]. Measuring species lifetime in units of addition attempts t , the lifetime distribution [Fig. 5(b), inset] is found to be broad, $\sim t^{-2}$, again consistent with the simple IEM [Eq. (1)].

Our results do not change qualitatively by varying r_{\min} , and in all cases the decay coefficients obtained progress infinitely towards ever smaller values. For larger values of r_{\min} it was numerically possible to reach a maximal level of species richness $S_{\max} \approx 2\beta/r_{\min}$. This value results when optimizing Eq. (2) for the maximal number of parallel two-species stacks (namely β/r_{\min}) corresponding to completely filling the two lowest trophic levels [19].

Figure 5(c) shows the species richness at different trophic levels corresponding to the simulation in Fig. 4(a). Noticeably, this distribution is independent of sampling time and largely independent of the assumed value of r_{\min} . Compared with assembled food webs [14], where a total number of 7–9 trophic levels was reached, the evolved food webs here are confined to usually less than five levels, with largest richness at the second level. The dynamics of this evolutionary “flattening” is mirrored by the relatively short species lifetimes at both levels 3 and 4 [Fig. 4(a) and Fig. 5(b), inset]. Thus species at levels three and above are systematically more prone to extinctions, reflecting their increased exposure and dependence on the species at lower levels.

The species richness distribution for seven empirically sampled food webs of free-living species is also limited to approximately four trophic levels [Fig. 5(d)]. The different trophic levels of these well-characterized [30–35] and recompiled [36,37] food webs have largest species richness at level 2 and only very few species at levels 5 and beyond. It should be pointed out that these empirical food webs presumably under-represent the richness at the basal level, as distinct species are often lumped into a single category there [15]. The remaining difference between our simulated food webs and empirical data is found at levels 3 and 4, which appear to be penalized too strongly by our assumed treelike topology: As they are assumed to feed on only one resource, top consumers become too dependent on extinction of “supply lines” provided by particular prey species. In empirical food webs there likely are several distinct nutrient or energy sources, e.g., sunlight and sugars, leading to larger breadth of the food webs these nutrients can support. Further, previous analysis of these empirical food webs suggests that omnivores and parasites may be prevalent [38,39] and possibly play important roles in stabilizing these ecosystem [15,36,40], characteristics not taken into account in our present model.

IV. DISCUSSION AND CONCLUSION

Within the comparably simple generalized Lotka-Volterra equations [Eqs. (2)–(6)], we studied hierarchical food webs, where each consumer has exactly one resource. While ide-

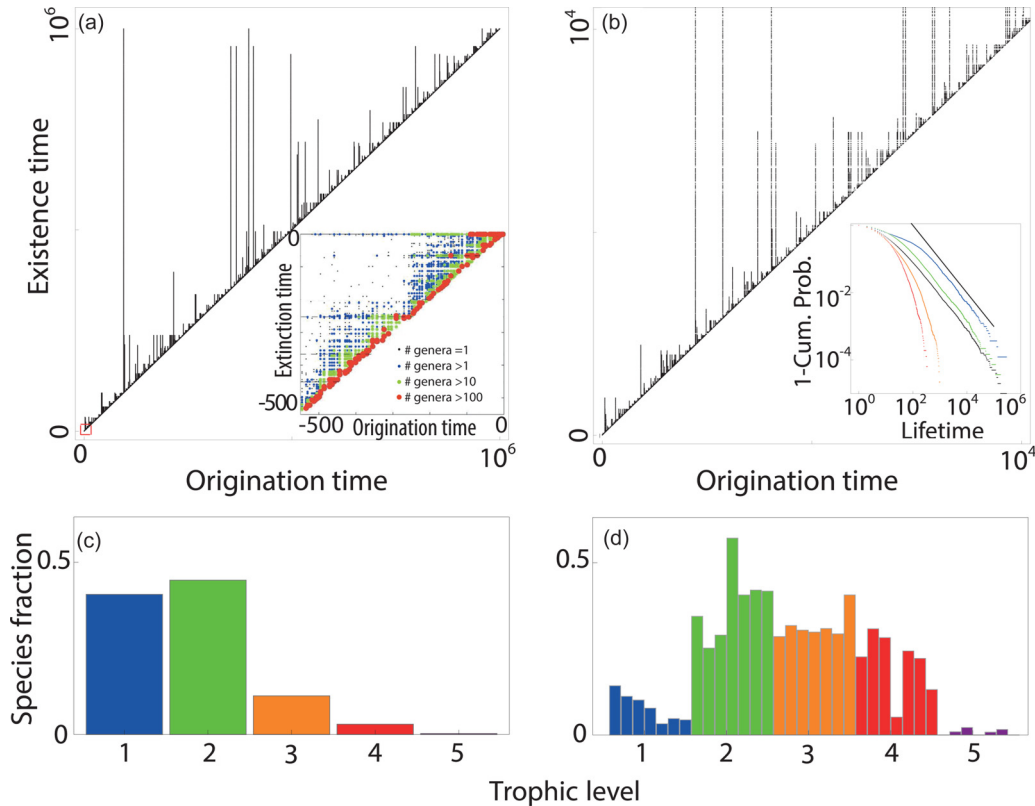


FIG. 5. Species origination and extinction. (a) Time evolution for 10^6 attempted species additions. Origination and existence time shown on horizontal and vertical axes, respectively. Inset: Origination-extinction matrix from fossil record data [28]; matrix reproduced from the literature [27,29]. (b) Magnification of the first 10^4 addition attempts, i.e., the region within the red box in the lower left corner of (a). Inset: Cumulative species lifetime distribution for each trophic level (blue to red for levels 1 to 4) and combined (black curve), the straight line indicates a power law with exponent -2 . (c) Average distribution of trophic levels for the data in Figs. 4(a) and 4(b). (d) Trophic levels obtained for the free-living species of seven high-resolution aquatic food web data sets [15].

alized, our approach can make the evolutionary dynamics of invasions and extinctions transparent by providing deterministic rules for extinction cascades caused by an invader. In reality, a species may in principle be connected to many others by consumption links. We, however, note that the strengths of links are by no means equal: In the field they are often found to even be bimodally distributed [41–44], meaning that feeding connections of a given consumer to its prey are dominated by one strong link. This feature is also seen in simulations [45,46] when assessing conditions for the growth of species-rich communities. We have previously explored by numerical simulations that adding sufficiently weak links (strength bounded by r_{\min}) to our constructed food webs does not generally lead to destabilization [14]. Further, in numerical work where food webs were assembled randomly [45], it was found that the ability of predators to prey on many different species generally limited the growth of multilevel food webs. Hence, models with few strong, but possibly many weak, links may be realistic. It was concluded that the impact of links either had to be weakened by nonlinear functional responses or the number of resource species had to be limited—a conclusion justified by the consideration of trade-off costs associated with the ability to generalize predation habits. Even though our methodology does not make any assumption on the interaction strength for the feeding links present, in our simulations we made an additional assumption for simplicity that they have

a similar magnitude. While this claim may be somewhat justified by the data as we discuss in Sec. A3, more work is needed to determine how much a nontrivial interaction strength distribution could alter the results.

Our simple two-level invasion-extinction model can in fact be seen as implementing the dynamics of an open system of multiple bacterial strains, each exposed to an exclusive phage predator. The states in the model correspond to a particular composition of an ecosystem of coexisting bacteria-phage pairs, obeying “kill the winner” equations [16]. Our model thereby speaks to the long-term evolution of such microbial ecosystems and when changes are governed by spatially separated systems with occasional emigration. Examples of such demographic systems are found in the ocean, where spatially separated samples have partly different bacteria-phage pairs [19,47].

Notably, the comparison with the kill-the-winner model underscores our assumption that, for a bacteria-phage ecology, each phage only preys on a unique bacterial strain, as this implies that the fastest-growing bacterial strain could only be replaced by an ever-faster-growing one. It is worth noting that the average number of prey strains per phage strain at a local station in the ocean data is 1.4 [19,47], i.e., the majority of phage strains have only one prey strain. Although this may often be the case, there is also the possibility that a phage strain preys on two bacterial strains, which for different adsorption

rates could then lead to the elimination of the fast grower [48]. This apparent competition was part of the more detailed microbial ecosystem model explored previously [19].

Our multilevel food web model allows invaders to aggressively compete with residents in an evolutionary process. The resulting simulated food webs are typically confined to the approximately four trophic levels that are typical of empirically sampled free-living species webs [38]. Compared to empirical food web data, our evolved treelike food webs underestimate species richness at trophic levels 3 and 4 and presumably overestimate stability of lower levels due to the simplified predation, where each invader only consumes a single prey species. We interpret these findings as hinting towards the possible necessity for greater link complexity at the higher trophic levels in order to achieve more realistic network structures there. Indeed, we found data collected from the field to show stronger preference towards omnivory and generalism at those levels [15]. Also parasitism has recently gained appreciation as a consumption form that may add to diversity [36]. The present methodology, including the IEM, may hence serve as benchmarks for more complex food web models, including those that involve nonlinear functional responses, omnivory, or parasitism.

Our models were limited to one feeding interaction per species. Thereby, the evolving system never reached a true steady state. Instead the “fittest” species tend to become increasingly robust as ever-lower decay rates r —or alternatively higher replication rates—are selected for. The erratic climbing towards improved r could, however, be arrested if one allowed for consumers to have two (or more) different resources that may have different values of interaction strength and consumption efficiency [α and β in Eqs. (5) and (6)]. In that case, apparent competition [49] between species [50] could cause the species of lower decay coefficient to be eliminated by the other through the mediated competition by a common consumer, as discussed as an effect of a keystone predator [51]. This type of dynamics would open for a steady-state “red queen” dynamics where relative fitness can increase also for the fittest species [19]. Such reshuffling has notably been discussed in models for coevolutionary avalanches [52,53]. Interestingly, the current analysis adds to these earlier and more coarse-grained models by pinpointing that changes in ecosystem composition can be indirect.

The prediction of a power law for species resident times in food webs makes it tempting to view our model in perspective of large-scale evolution. In particular, the species lifetime of $\propto 1/t^2$ is compatible with species longevity distributions in the fossil record [27]. Also the current model implies cascades of extinctions that superficially resemble those of Bak and Sneppen [52], but the current cascades are typically small and exponentially distributed with a characteristic size of unity. Thus our model does not speak directly to the large extinction events in the palaeontological history [54,55]. Rather, the cascades in the IEM may potentially take the role of the fast and small neighborhood changes envisioned in the avalanche scenario proposed by Bak and Sneppen [52].

Finally, the treelike food webs we analyzed highlight a new interplay between a species’ trophic level, its robustness against extinctions, and its ability to compensate by diversifying its food sources. Without compensatory food sources,

species at higher trophic levels will more easily be exposed to perturbations from their prey or the preys’ prey and thus be expected to suffer shorter existence times. It is therefore noteworthy that species at higher trophic levels as well as species with large body size or more specialized diets are often cited to have relatively high species extinction rates in both the fossil record and among modern extinctions [56].

ACKNOWLEDGMENTS

The authors acknowledge the financial support of the European Research Council under the European Union’s Seventh Framework Programme (FP/2007 2013)/ERC Grant No. 740704. N.M. is supported by the Danish National Research Foundation through the Center for Bacterial Stress Response and Persistence (DNRF120). J.O.H. acknowledges support by a research grant (Grant No. 13168) from VILLUM FONDEN.

APPENDIX

1. Distribution of decay coefficients in the iem

We analyze the ensemble-averaged distribution of decay coefficients $\Delta r \equiv r - r_{\min}$. Suppose that, at time t , there are $S(r,t)dr$ numbers r_i , $i \in \{1, \dots, S(r,t)\}$, that satisfy $r < r_i < r + dr$. We define the cumulative distribution as $C(r,t) = \int_r^1 S(r',t)dr'$, namely $S(r,t) = -\frac{\partial}{\partial r} C(r,t)$.

Since $C(r,t+1)$ is zero with probability $(r - r_{\min})/(1 - r_{\min})$, and if the new random number takes a value between r' and $r' + dr'$ with $r < r' < 1$, then $C(r,t+1)$ will become $C(r,t) - C(r',t) + 1$. We have

$$\begin{aligned} C(r,t+1) &= \left(\frac{1}{1-r_{\min}}\right) \int_r^1 [C(r,t) - C(r',t) + 1]dr \\ &= \left(\frac{1}{1-r_{\min}}\right) \left[(1-r)C(r,t) - \int_r^1 C(r',t)dr' \right. \\ &\quad \left. + (1-r) \right]. \end{aligned}$$

Approximating $C(r,t+1) - C(r,t) \approx \frac{\partial}{\partial t} C(r,t)$ and taking the derivative with respect to r , we have

$$-\frac{\partial}{\partial t} S(r,t) = \frac{r - r_{\min}}{1 - r_{\min}} S(r,t) - \frac{1}{1 - r_{\min}}. \quad (\text{A1})$$

Integrating Eq. (A1) under the initial condition $S(r,0) = 0$, we finally obtain

$$\begin{aligned} S(r,t) &= \frac{1}{\Delta r} \left[1 - \exp\left(-\frac{\Delta r}{1 - r_{\min}} t\right) \right] \\ &\approx \frac{1}{\Delta r} [1 - \exp(-\Delta r t)], \end{aligned}$$

where $r_{\min} \ll 1$ was assumed.

Note that this distribution shows a slower relaxation when r approaches its lower threshold $r \rightarrow r_{\min}$, i.e., $\Delta r \rightarrow 0$. For $t \gg 1/\Delta r$, the probability distribution function of Δr is a power law with slope 1, and we have $C(r,t) \approx -\log(\Delta r)$, i.e., $\Delta r \approx e^{-C}$. At the same time, $C(r,t)$ denotes the extinction size when the new species has a decay rate r . This gives the

avalanche size distribution to be

$$P(C) \approx \left| \frac{d\Delta r}{dC} \right| \approx e^{-C}.$$

2. Collective decay rates

The collective decay rate is defined recursively from the top species of the branch as $r_{\text{coll},c}^{(l)} = r_{\text{eff},c}^{(l)} + r_{\text{coll},f}^{(l+1)}/\beta^{(l)}$, for a controlled species, where $r_{\text{coll},f}^{(l+1)}$ is the collective decay rate of the paired free species, while for a free species, we have $r_{\text{coll},f}^{(l)} = \max[r_{\text{coll},c}^{(l+1)}]$, where the maximum is taken by comparing the collective decay rates of all the controlled species preying on the considered free species.

This rule is easily understood when considering part of the food web that constitutes a chain and feeds on a controlled

species [as in Fig. 3(c,III), side branch]. Suppose the branching point is at the trophic level $l - 1$ and its population is determined by the effective decay rate of the invading free species at the level l as $N^{*(l-1)} = \tilde{r}_{\text{eff}}$. The top species of the side controlled branch should be at level $l + 2n + 1$ with a positive integer n . The energy flux for the controlled species at the level $l + 2m$ in this branch will then be

$$w^{(l+2m)}(\mathbf{N}) = \beta^{(l+2m)} [N^{(l+2m-1)} - r_{\text{eff},c}^{(l+2m)}] - N^{(l+2m+1)}.$$

By setting this to be zero, the steady-state biomass of the free species in the side chain will be determined by $N_f^{*(l+2m+1)} = \beta^{(l+2m)} [N^{*(l+2m-1)} - r_{\text{eff},c}^{(l+2m)}]$. Recursively, this determines the biomass of the free top species as

$$\begin{aligned} N_f^{*(l+2n+1)} &= \beta^{(l+2n)} [N^{*(l+2n-1)} - r_{\text{eff},c}^{(l+2n)}] = \beta^{(l+2n)} \{ \beta^{(l+2n-2)} [N^{*(l+2n-3)} - r_{\text{eff},c}^{(l+2n-4)}] - r_{\text{eff},c}^{(l+2n)} \} \\ &= \dots = \prod_{k=0}^n \beta^{(l+2k)} [N^{*(l-1)} - r_{\text{eff},c}^{(l)}] - \prod_{k=1}^n \beta^{(l+2k)} r_{\text{eff},c}^{(l+2)} - \dots - \beta^{(l+2n)} r_{\text{eff},c}^{(l+2n)}. \end{aligned}$$

Thus the condition for the positive biomass for the top species ($N_f^{*(l+2n+1)} > 0$) gives

$$\begin{aligned} \tilde{r}_{\text{eff}} &> r_{\text{eff},c}^{(l)} + (1/\beta^{(l)}) r_{\text{eff},c}^{(l+2)} \dots + \prod_{k=0}^{n-1} [1/\beta^{(l+2k)}] r_{\text{eff}}^{(l+2n)} \\ &= r_{\text{coll},c}^{(l)}. \end{aligned} \quad (\text{A2})$$

Namely, one should compare the sum of decay rates of the controlled species in the side chain, which should be divided by β as it goes down from the top species population.

3. Realistic values of consumption efficiency

The data we present focus on the consumption efficiency $\beta^{(l)} = 1$ in the dimensionless form multiplied by the ratio of interaction strength $\alpha^{(l,l-1)}/\alpha^{(l-1,l-2)}$ in successive trophic levels. The value of α is difficult to evaluate, but studies [42,57] report the percapita negative effect of predator on prey to decrease by an order of magnitude with trophic position.

This number can be interpreted as $\alpha^{(l,l-1)}$ multiplied by the steady-state biomass of prey at the trophic level $l - 1$, while the biomass decreases on average an order of magnitude for higher trophic levels [42,57]. Thus, the simplest assumption of $\alpha^{(l,l-1)}/\alpha^{(l-1,l-2)} \sim 1$ is reasonably consistent with these data. Assuming this, the conversion efficiency in real food webs are still expected to be substantially smaller than 1, approximately $\beta \sim 0.1$. Given that we are working with relatively few trophic levels, a general decrease in efficiency can be compensated by a proportional decrease in decay coefficients (r), while giving similar species richness distributions for the different trophic levels. Further, the potential decay coefficients for larger animals at higher food web levels should be systematically lower than for many of the smaller-sized bottom feeders. Overall, we therefore find that our prediction of a maximal food web level of about 4 is robust to realistic variation of parameters.

- [1] S. Díaz, J. Fargione, F. S. Chapin III, and D. Tilman, *PLoS Biol.* **4**, e277 (2006).
- [2] M. Lenzen, D. Moran, K. Kanemoto, B. Foran, L. Lobefaro, and A. Geschke, *Nature* **486**, 109 (2012).
- [3] N. Bax, A. Williamson, M. Agüero, E. Gonzalez, and W. Geeves, *Mar. Policy* **27**, 313 (2003).
- [4] J. Gurevitch and D. K. Padilla, *Trends Ecol. Evol.* **19**, 470 (2004).
- [5] J. G. Ehrenfeld *et al.*, *Annu. Rev. Ecol. Evol. Systemat.* **41**, 59 (2010).
- [6] A. Ricciardi, M. F. Hoopes, M. P. Marchetti, and J. L. Lockwood, *Ecol. Monogr.* **83**, 263 (2013).
- [7] G. A. Polis, A. L. Sears, G. R. Huxel, D. R. Strong, and J. Maron, *Trends Ecol. Evol.* **15**, 473 (2000).
- [8] M. Clavero, L. Brotons, P. Pons, and D. Sol, *Biol. Conserv.* **142**, 2043 (2009).
- [9] M. R. Heath, D. C. Speirs, and J. H. Steele, *Ecol. Lett.* **17**, 101 (2014).
- [10] K. S. McCann, *Nature* **405**, 228 (2000).
- [11] G. Gause, *Soil Sci.* **41**, 159 (1936).
- [12] G. Hardin, *Science* **131**, 1292 (1960).
- [13] J. P. Grover, *Resource Competition*, Vol. 19 (Springer Science & Business Media, Berlin, 1997).
- [14] J. O. Haerter, N. Mitarai, and K. Sneppen, *Phys. Rev. E* **96**, 032406 (2017).
- [15] J. O. Haerter, N. Mitarai, and K. Sneppen, *PLoS Comput. Biol.* **12**, e1004727 (2016).
- [16] T. F. Thingstad, *Limnol. Oceanogr.* **45**, 1320 (2000).
- [17] J. S. Weitz, H. Hartman, and S. A. Levin, *Proc. Natl. Acad. Sci. USA* **102**, 9535 (2005).
- [18] L. Childs, N. Held, M. Young, R. Whitaker, and J. Weitz, *Evolution* **66**, 2015 (2012).

- [19] J. O. Haerter, N. Mitarai, and K. Sneppen, *ISME J.* **8**, 2317 (2014).
- [20] Y. Iwasa, F. Michor, and M. Nowak, *J. Theor. Biol.* **229**, 179 (2004).
- [21] S. Johnson, V. Domínguez-García, L. Donetti, and M. A. Muñoz, *Proc. Natl. Acad. Sci. USA* **111**, 17923 (2014).
- [22] J. Hofbauer and K. Sigmund, *The Theory of Evolution and Dynamical Systems* (Cambridge University Press, Cambridge, 1988), p. 59ff.
- [23] B. Drossel and A. J. McKane, in *Handbook of Graphs and Networks*, edited by S. Bornholdt and H. G. Schuster (Wiley-VCH, New York, 2003), pp. 218–247.
- [24] R. Levins, in *Ecology and Evolution of Communities*, edited by M. L. Cody and M. D. Jared (Harvard University Press, 1975), Chap. 1.
- [25] D. Tilman, *Resource Competition and Community Structure* (Princeton University Press, Princeton, NJ, 1982).
- [26] R. H. MacArthur, *Geographical Ecology: Patterns in the Distribution of Species* (Princeton University Press, Princeton, NJ, 1972).
- [27] S. Bornholdt, K. Sneppen, and H. Westphal, *Theor. Biosci.* **128**, 75 (2009).
- [28] J. J. Sepkoski Jr., *Paleobiology* **19**, 43 (1993).
- [29] K. Sneppen, *Models of Life* (Cambridge University Press, Cambridge, 2014).
- [30] R. F. Hechinger, K. D. Lafferty, J. P. McLaughlin, B. L. Fredensborg, T. C. Huspeni, J. Lorda, P. K. Sandhu, J. C. Shaw, M. E. Torchin, K. L. Whitney *et al.*, *Ecology* **92**, 791 (2011).
- [31] K. D. Lafferty, A. P. Dobson, and A. M. Kuris, *Proc. Natl. Acad. Sci. USA* **103**, 11211 (2006).
- [32] C. D. Zander, N. Josten, K. C. Detloff, R. Poulin, J. P. McLaughlin, and D. W. Thieltges, *Ecology* **92**, 2007 (2011).
- [33] D. W. Thieltges, K. Reise, K. N. Mouritsen, J. P. McLaughlin, and R. Poulin, *Ecology* **92**, 2005 (2011).
- [34] K. N. Mouritsen, R. Poulin, J. P. McLaughlin, and D. W. Thieltges, *Ecology* **92**, 2006 (2011).
- [35] M. Huxham, S. Beaney, and D. Raffaelli, *Oikos* **76**, 284 (1996).
- [36] J. A. Dunne, K. D. Lafferty, A. P. Dobson, R. F. Hechinger, A. M. Kuris, N. D. Martinez, J. P. McLaughlin, K. N. Mouritsen, R. Poulin, K. Reise *et al.*, *PLoS Biol.* **11**, e1001579 (2013).
- [37] J. A. Dunne *et al.* (private communication).
- [38] R. J. Williams and N. D. Martinez, *Am. Nat.* **163**, 458 (2004).
- [39] R. M. Thompson, M. Hemberg, B. M. Starzomski, and J. B. Shurin, *Ecology* **88**, 612 (2007).
- [40] W. F. Fagan, *Am. Nat.* **150**, 554 (1997).
- [41] R. T. Paine, *Nature* **355**, 73 (1992).
- [42] P. C. de Ruiter, A.-M. Neutel, and J. C. Moore, *Science* **269**, 1257 (1995).
- [43] J. T. Wootton and M. Emmerson, *Annu. Rev. Ecol. Evol. Systemat.* **419** (2005).
- [44] K. T. Allhoff and B. Drossel, *J. Theor. Biol.* **334**, 122 (2013).
- [45] B. Drossel, A. J. McKane, and C. Quince, *J. Theor. Biol.* **229**, 539 (2004).
- [46] C. Quince, P. G. Higgs, and A. J. McKane, *Ecol. Model.* **187**, 389 (2005).
- [47] K. Moebus and H. Nattkemper, *Helgol. Meeresunt.* **34**, 375 (1981).
- [48] J. O. Haerter and K. Sneppen, *mBio* **3**, e00126-12 (2012).
- [49] R. D. Holt, *Theoret. Popul. Biol.* **12**, 197 (1977).
- [50] S. Wollrab, S. Diehl, and A. M. Roos, *Ecol. Lett.* **15**, 935 (2012).
- [51] M. A. Leibold, *Am. Nat.* **147**, 784 (1996).
- [52] P. Bak and K. Sneppen, *Phys. Rev. Lett.* **71**, 4083 (1993).
- [53] R. V. Solé and S. C. Manrubia, *Phys. Rev. E* **54**, R42 (1996).
- [54] D. Jablonski, *Science* **253**, 754 (1991).
- [55] D. M. Raup, *Extinction: Bad Genes or Bad Luck?* (W. W. Norton & Company, New York, 1992).
- [56] M. L. McKinney, *Annu. Rev. Ecol. Systemat.* **28**, 495 (1997).
- [57] A.-M. Neutel, J. A. Heesterbeek, and P. C. de Ruiter, *Science* **296**, 1120 (2002).